

Spontaneous autoimmunity prevented by thymic expression of a single self-antigen

Jason DeVoss,¹ Yafei Hou,² Kellsey Johannes,¹ Wen Lu,¹ Gregory I. Liou,³ John Rinn,⁴ Howard Chang,⁴ Rachel Caspi,⁵ Lawrence Fong,² and Mark S. Anderson^{1,2}

¹Diabetes Center and ²Department of Medicine, University of California, San Francisco, San Francisco, CA 94143

³Department of Ophthalmology, Medical College of Georgia, Augusta, GA 30912

⁴Cancer Biology Program, Stanford University School of Medicine, Stanford, CA 94305

⁵Laboratory of Immunology, National Eye Institute, National Institutes of Health (NIH), Bethesda, MD 20892

The expression of self-antigen in the thymus is believed to be responsible for the deletion of autoreactive T lymphocytes, a critical process in the maintenance of unresponsiveness to self. The *Autoimmune regulator (Aire)* gene, which is defective in the disorder autoimmune polyglandular syndrome type 1, has been shown to promote the thymic expression of self-antigens. A clear link, however, between specific thymic self-antigens and a single autoimmune phenotype in this model has been lacking. We show that autoimmune eye disease in *aire*-deficient mice develops as a result of loss of thymic expression of a single eye antigen, interphotoreceptor retinoid-binding protein (IRBP). In addition, lack of IRBP expression solely in the thymus, even in the presence of *aire* expression, is sufficient to trigger spontaneous eye-specific autoimmunity. These results suggest that failure of thymic expression of selective single self-antigens can be sufficient to cause organ-specific autoimmune disease, even in otherwise self-tolerant individuals.

CORRESPONDENCE

Mark Anderson:
manderson@diabetes.ucsf.edu

Abbreviations used: Aire, autoimmune regulator; APECED, autoimmune polyendocrinopathy candidiasis ectodermal dystrophy; DKO, double knockout; EAU, experimental autoimmune uveitis; IRBP, interphotoreceptor retinoid-binding protein; mTEC, medullary thymic epithelial cell; PMF, peptide mass fingerprinting; S-Ag, retinal soluble antigen; TSA, tissue-specific self-antigen.

Autoimmunity results from a breakdown in immune tolerance, a phenomenon that can occur in both the central (generative) lymphoid organs and peripheral tissues. Within the thymus, it has clearly been established that expression of self-antigens can mediate the deletion of self-reactive T cells (1, 2). However, to our knowledge there exists no direct evidence that thymic selection against a single self-antigen is essential in preventing a spontaneous organ-specific autoimmune disease from occurring. Recently, the possibility of providing evidence of this mechanism has been afforded by the detailed study of the *autoimmune regulator (Aire)* gene (3, 4). Aire is a putative transcription factor that was identified through a positional cloning effort in human subjects with the monogenic recessive disorder autoimmune polyendocrinopathy candidiasis ectodermal dystrophy (APECED) (5, 6). APECED patients develop autoimmune infiltrates in multiple organs and autoantibodies to multiple organ-specific antigens (7). Like APECED subjects, *aire*-deficient mice spontaneously develop multiple organ infiltrates and autoantibodies

(3, 8–10). Experiments with the mouse model have shown that a defect in the thymus is sufficient for the development of the autoimmune syndrome (3, 9). Within the thymus, Aire's expression mainly localizes to a subset of medullary thymic epithelial cells (mTECs) that have been shown to ectopically express many tissue-specific self-antigens (TSAs) (11). It appears that Aire is involved in driving the expression of a subset of these TSAs in mTECs, leading to a working model in which Aire prevents autoimmunity by promoting the deletion of potentially self-reactive thymocytes with specificity for the Aire-regulated TSAs (3, 4, 12). Detailed analyses of the *aire*-regulated TSAs in mTECs using microarrays suggests that *aire* controls the expression of a wide array of self-antigens (3, 13). However, the scope and number of antigens that are critical for preventing any individual autoimmune disease phenotype in this model is unknown.

To further clarify how the loss of *aire* function leads to one of the spontaneously occurring autoimmune phenotypes in the mouse model, we sought to clearly define the targeted antigens, whether such antigens are primary or secondary targets, and whether the targeted

The online version of this article contains supplemental material.

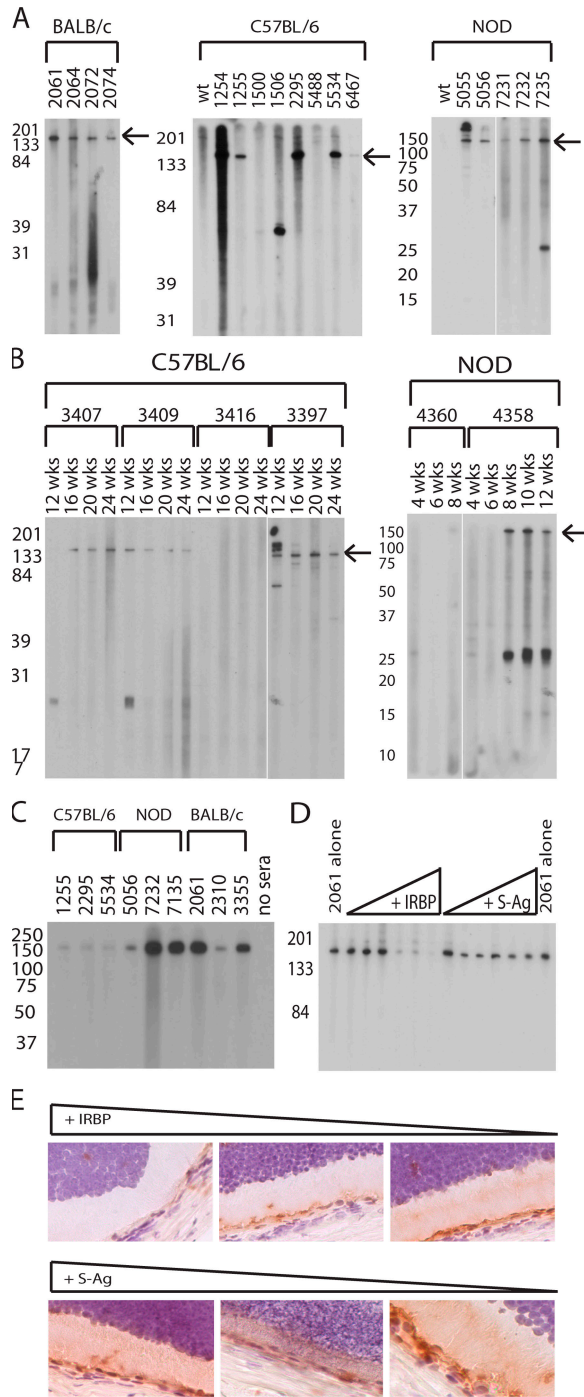


Figure 1. Aire-deficient mice have a limited autoreactive repertoire and predominantly recognize IRBP. (A) Immunoblotting of whole-eye extracts with aire-deficient (individual animals listed by number) and strain- and age-matched wild types for BALB/c, C57BL/6, and NOD mice. (B) C57BL/6 and NOD aire-deficient animals were bled by tail vein at various time points, and sera were immunoblotted against whole-eye extracts to determine kinetic changes in autoantibody reactivity. Arrows in A and B indicate the IRBP band. (C) Purified, full-length bovine IRBP was immunoblotted with sera derived from aire-deficient animals. (D) Sera from individual animals were preincubated with bovine IRBP or S-Ag before use as primaries in an immunoblot against whole-eye extract. S-Ag,

antigen is expressed in the thymus and is aire regulated. For this, we chose to perform a detailed analysis of the autoimmune disease that occurs in the posterior portion of the eye in aire-deficient animals as a representative model. Aire-deficient mice develop spontaneous immune infiltrates in the posterior chamber of the eye that are reminiscent of those seen in the induced rodent model of experimental autoimmune uveitis (EAU) (3, 14, 15), and APECED patients have also been described that develop idiopathic retinopathy (16). In this paper, we demonstrate that the eye disease that spontaneously develops in aire-deficient mice is targeted against a single antigen whose expression is controlled within the thymus by aire. In addition, we also show that the expression of this single eye antigen within the thymus is critical to prevent spontaneous autoimmunity against the eye, even in the presence of functional aire.

RESULTS

Aire-deficient mice have a limited autoreactive repertoire to eye antigens

We had previously shown that aire-deficient animals develop a spontaneous autoimmune uveitis that increases in frequency and severity with age and is characterized by a mononuclear infiltrate and autoantibodies specific to the photoreceptor layer of the retina (3). These autoantibodies were used as a tool to define the specificity of the immune response. To determine the complexity of the eye-specific autoantibody repertoire, whole-eye extract was immunoblotted with sera from a large number of aged aire-deficient mice from several genetic backgrounds (Fig. 1 A and Fig. S1, available at <http://www.jem.org/cgi/content/full/jem.20061864/DC1>) (9). Many sera derived from individual aire-deficient mice reacted strongly against an antigen migrating at 150 kD; however, some variability was observed within and between strains. To help distinguish the primary targets of the immune response, kinetic studies were also performed. In both the NOD and C57BL/6 (B6) strains, we observed that reactivity against the 150-kD antigen generally develops at the same time or before any other reactivities (Fig. 1 B).

The predominant eye autoantigen is interphotoreceptor retinoid-binding protein (IRBP)

To identify this 150 kD antigen, immunoprecipitation was performed on columns containing protein agarose coupled to knockout animal sera (17). Tissue extracts were precleared to identify nonspecific background with columns coupled to wild-type animal sera. Eluates from both wild-type and aire-deficient sera-coupled columns were concentrated and subjected to immunoblotting. The immunoprecipitation eluate from the aire-deficient but not the wild-type coupled column

another photoreceptor-specific antigen, was included as a control. (E) Sera preincubated with bovine IRBP or S-Ag were also used for immunohistochemistry and visualized with DAB chromogen.

had a band observable by coomassie stain that, when immunoblotted with aire-deficient sera, had strong reactivity at 150 kD (Fig. S2, available at <http://www.jem.org/cgi/content/full/jem.20061864/DC1>). This 150-kD band from the aire-deficient eluate was given a provisional identification by peptide mass fingerprinting (PMF) as IRBP (Fig. S3). IRBP is a photoreceptor-specific antigen with the appropriate molecular mass for our candidate (~150 kD) that is known to bind retinoids, and its expression is localized to the photoreceptor matrix of the retina between the retinal pigment epithelium and the photoreceptor cells (18). IRBP is also a known autoantigen; i.e., an emulsification of full-length bovine IRBP in adjuvant can elicit EAU in rodents (15, 18).

To confirm that IRBP was the 150-kD target antigen, purified full-length bovine IRBP was immunoblotted with aire-deficient sera. Reactivity against bovine IRBP was observed in all strains tested: B6, NOD, BALB/c (Fig. 1 C), and (B6 × NOD)F2 (Fig. S1). When purified bovine IRBP was incubated with aire-deficient sera before immunoblotting, reactivity against the 150-kD band in whole mouse eye extract was diminished (Fig. 1 D). In contrast, incubation with an equal concentration of purified retinal soluble antigen (S-Ag), another photoreceptor-specific protein, failed to abrogate reactivity. This competition was similarly observed on frozen sections stained with aire-deficient sera (Fig. 1 E). Finally, indirect immunofluorescence using sera from aire-deficient mice on IRBP-deficient eye sections failed to recapitulate the photoreceptor-specific autoantibody reactivity observed previously (Fig. S4, available at <http://www.jem.org/cgi/content/full/jem.20061864/DC1>) (3). From these experiments, we conclude that IRBP is a dominant autoantigen targeted by autoantibodies in the spontaneous autoimmune uveitis observed in aire-deficient animals.

Uveitis in aire-deficient mice is T cell dependent

Although autoantibodies against IRBP predominate in aire-deficient mice, previous work has demonstrated that reconstitution of athymic nude mice with aire-deficient thymi is sufficient to induce the eye disease, thus implicating auto-reactive T cells as effectors in the disease process (3, 9). To further characterize the cellular requirements for disease, we analyzed the infiltrates of aire-deficient animals with uveitis. Using immunohistochemistry with antibodies against cell-surface markers, we determined that CD4⁺ T cells make up the bulk of infiltrating immune cells within the retina, although both CD8⁺ T cells and IgD-expressing B cells were also observed (Fig. 2 A). As a control, age-matched aire-sufficient NOD mice were analyzed (Fig. 2 B), and no infiltrates were observed. To determine which cellular subset was capable of transferring disease, specific cell populations were adoptively transferred into immunodeficient NOD.*scid* host mice. Spleen and cervical lymph node cells were pooled (Fig. 2 C), depleted of either CD4⁺ or CD8⁺ T cell subsets, and adoptively transferred into immunodeficient animals (Table S1, available at <http://www.jem.org/cgi/content/full/jem.20061864/DC1>). Animals that received CD4⁺ T-depleted

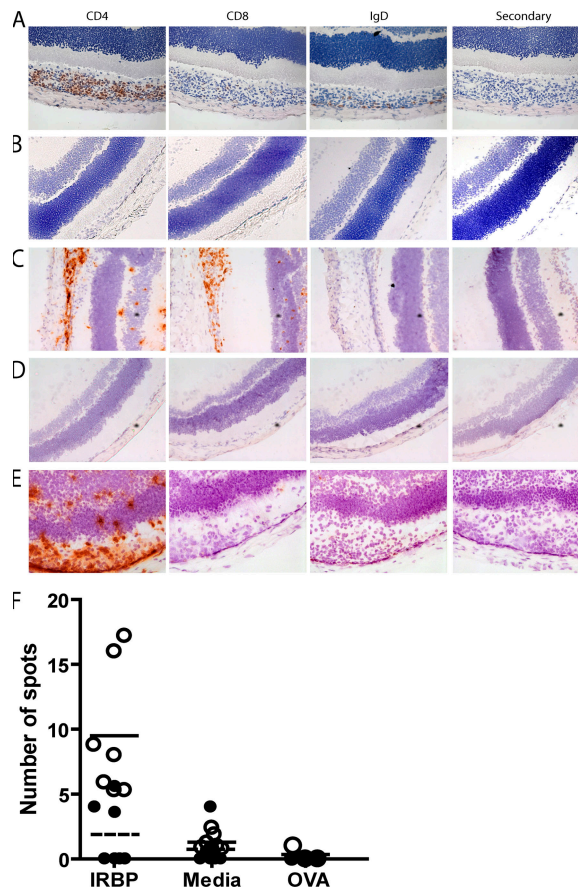


Figure 2. Uveitis in aire-deficient animals is T cell dependent, and increased frequencies of IRBP-specific T cells arise in aire-deficient animals. Immunostaining of frozen eye sections from aire-deficient mice with cell surface markers identifies CD4⁺ T cells as the predominant cells within the mononuclear infiltrate. (A) CD8⁺ T cells and IgD⁺ B cells are also present in the retina. (B) No infiltrate was observed in the eyes of age-matched, aire-sufficient animals. (C) Eye disease can be transferred with a pooled population of splenocytes and cervical lymph node cells from aire-deficient animals. Cells devoid of (E) CD8⁺ T cells but not (D) CD4⁺ T cells are capable of transferring disease into immunodeficient hosts. T cells were purified from cervical lymph nodes from unimmunized aire-deficient and age- and sex-matched aire wild-type controls in the C57BL/6 background (18–20 wk old). (F) T cells were assayed in an ELISPOT assay for IFN- γ production in the presence of 10 μ g/ml IRBP, media alone, or 10 μ g/ml OVA in the presence of APCs (ConA was also tested as a positive control; not depicted). Open circles represent individual aire-deficient animals; the solid line indicates the mean value. Closed circles represent individual aire-sufficient animals; the dashed line indicates the mean value. For IRBP and media alone, $n = 7$ animals per group; the number of spots for IRBP was statistically significant ($P = 0.0023$) for aire-deficient compared with aire-sufficient animals. For the OVA control, $n = 3$ animals per group.

cell populations failed to develop eye disease or autoantibodies (Fig. 2 D and not depicted). In contrast, animals that received CD8⁺ T-depleted cells developed disease and photoreceptor-specific autoantibodies that reacted against IRBP (Fig. 2 E and not depicted).

We next asked whether *aire*-deficient mice had an increased precursor frequency of IRBP-reactive CD4⁺ T cells. T cells were isolated from *aire*-sufficient or *aire*-deficient animals and cultured with APCs loaded with purified bovine IRBP. ELISPOT analysis of T cells reacting against these IRBP-loaded APCs (or OVA as a control antigen) showed that *aire*-deficient mice had an increased frequency of IRBP-reactive cells in their immune repertoire (Fig. 2 F). Previous work has suggested that *aire*-deficient dendritic cells may cause T cell hyperproliferation (19). Thus, as an additional control, experiments were performed in which purified T cells from *aire*-deficient or *aire*-sufficient mice were mixed only with *aire*-sufficient irradiated splenocytes as a source of APCs. Again, we observed increased reactivity to IRBP in *aire*-deficient mice (Fig. S5, available at <http://www.jem.org/cgi/content/full/jem.20061864/DC1>).

IRBP expression in the thymus is aire dependent

Having identified the ocular autoantigen targeted in *aire*-deficient mice and characterized the cells involved, we next sought to confirm that IRBP is expressed in the thymus (20) and to determine whether or not its thymic expression is *aire* regulated. We purified thymic stroma from *aire*-sufficient and *aire*-deficient mice and generated cDNA from these cells. Using this cDNA, we queried several known *aire*-regulated and *aire*-independent TSAs, as well as IRBP, using quantitative real-time PCR. Indeed, IRBP was found to be expressed in the thymus, and the thymic expression of IRBP was found to be *aire*-dependent in our analysis (Fig. 3 A). Importantly, the expression of insulin, a known *aire*-regulated antigen (3), was observed in *aire*-sufficient but not *aire*-deficient

thymic stroma, whereas GAD67, which is not *aire* regulated (3), was equally expressed in both cell samples. Interestingly, the expression of IRBP within these cells was quite low: although the Ct for cyclophilin, a housekeeping control, was approximately equal for both pools of cells (average Ct = 22.2 for *aire*-sufficient cells and 21.9 for *aire*-deficient cells; Fig. 3 B), the Ct of IRBP was almost at the limit of detection (Ct = 38.2 for *aire*-sufficient cells and not detectable in *aire*-deficient cells; Fig. 3 C).

However, IRBP is not the only retina-specific gene regulated by *aire* in the thymus. To identify other potential retinal autoantigens that are *aire*-regulated in the thymus, we generated a list by compiling publicly available gene chip datasets that examine *aire*-deficient versus *aire*-sufficient mTEC gene expression (3, 13) and gene chip datasets identifying retinal expressed genes (Fig. 3 E) (21). In an attempt to confirm that these genes were in fact *aire* regulated, we used real-time PCR to study the expression of four of these genes in thymic stroma from *aire*-sufficient and *aire*-deficient mTECs. Two of these four genes were down-regulated >75% in the *aire*-deficient compared with the *aire*-sufficient thymic stroma (Fig. 3 F), showing that at least a subset of the genes on this list are *aire* regulated within the thymus.

Uveitis in aire-deficient mice is IRBP dependent

In an effort to prove that the uveitic process in *aire*-deficient mice is directly dependent on IRBP and that reactivity does not result from a secondary process like epitope spreading, we obtained IRBP-deficient mice and performed a genetic test cross with *aire*-deficient mice. Importantly, IRBP-deficient mice maintain a retina structure that has minor changes,

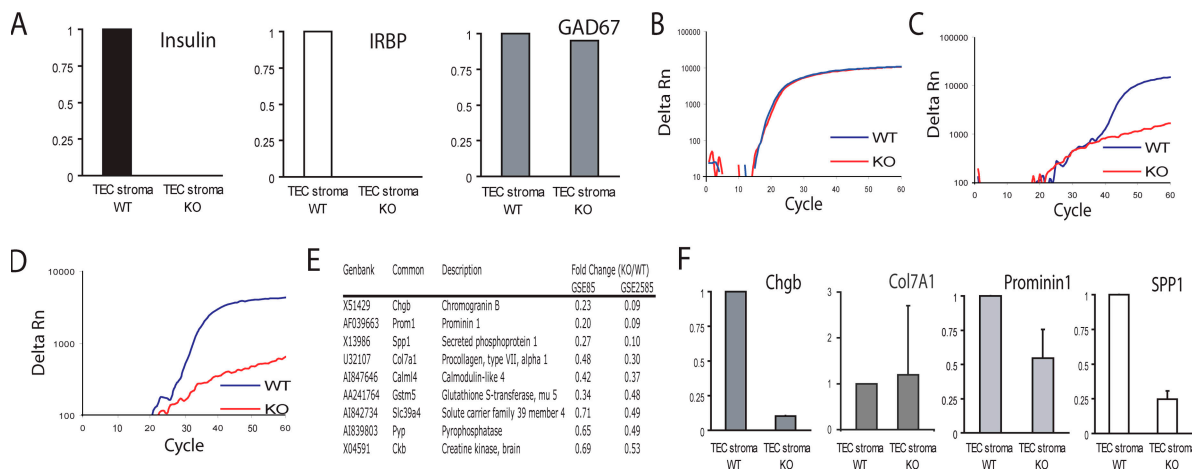


Figure 3. IRBP is an *aire*-regulated antigen expressed in the thymus.

(A) cDNA derived from thymic stroma of *aire*-deficient and *aire*-sufficient animals was prepared. Quantitative real-time PCR was used to determine the expression of known TSAs (insulin and Gad67) and IRBP. Values are normalized to cyclophilin and are relative to expression in the WT TEC stroma. Data represent the mean of three independent experiments. A representative amplification plot of (B) cyclophilin, (C) IRBP, and (D) insulin are shown for wild-type and *aire*-deficient thymic stroma.

(E) Summaries of genes shown in two publicly available datasets, GSE85 (reference 3) and GSE2585 (reference 13), to be *aire*-regulated in the thymus were each queried for retinal-expressed transcripts. The top nine transcripts fitting this profile are shown (all statistically significant; P < 0.05). (F) Quantitative real-time PCR was used to confirm the expression of the microarray-identified genes. Values are normalized to cyclophilin and are relative to expression in the WT TEC stroma. Error bars represent mean ± SD.

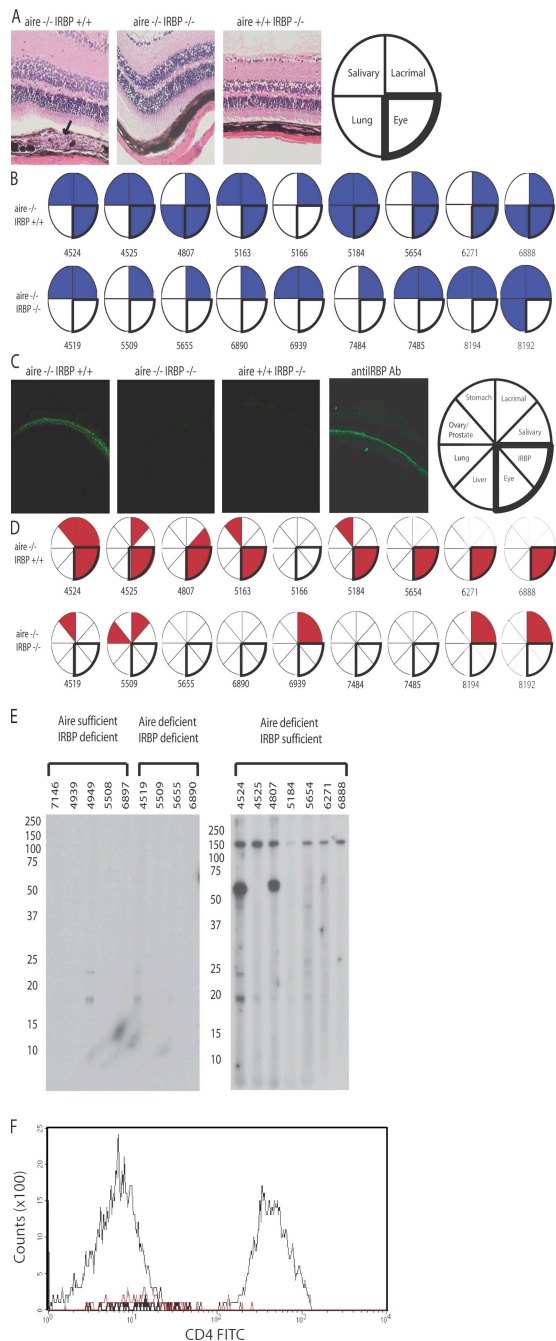


Figure 4. Uveitis in *aire*-deficient animals is IRBP dependent. The *aire* mutation was bred with IRBP-deficient animals (both backcrossed >10 generations back to C57BL/6) to produce animals devoid of *aire* and IRBP expression. 18–20-wk-old DKO and *aire* single knockouts were analyzed for disease. (A) *Aire* single knockouts, but not DKOs, displayed a characteristic mononuclear cell infiltrate (indicated with an arrow) in the retina, as shown in representative histology from the indicated groups. However, both sets of animals showed infiltrates in numerous other organs, as described for *aire*-deficient mice. (B) Blue-shaded sections of the pie graphs indicate the presence of mononuclear infiltrates in the designated organ, and each circle and corresponding number represent an individual mouse for that group. (C) Similarly, *aire* single knockouts, but not DKOs, displayed an autoantibody reactivity to the photoreceptor cell

including some thinning of the outer nuclear layer (22). Consistent with a dominant role for IRBP, aged mice deficient for both *aire* and IRBP (double knockout; DKO) do not have mononuclear infiltrates within the retina ($P = 0.0006$; Fig. 4 A), nor are they capable of generating autoantibodies against the photoreceptor layer (Fig. 4 C). As observed in previously published data, not all C57BL/6 *aire*-deficient animals manifest ocular autoimmunity (3, 10). A small percentage of *aire*-deficient animals on the C57BL/6 background are free of infiltrates and autoantibodies specific for the 150-kD band, purified bovine IRBP, or the photoreceptor layer as determined by immunoblotting and indirect immunofluorescence, respectively (Fig. 4, B and D, animal 5166; and Fig. S6, available at <http://www.jem.org/cgi/content/full/jem.20061864/DC1>). In contrast, all DKO mice analyzed to date ($n = 10$) fail to develop not only IRBP-specific autoantibodies but also other reactivities directed at the eye that arise in *aire*-deficient mice (Fig. 4, D and E). Thus, in the absence of IRBP, no ocular antigens are targeted by autoantibodies. Importantly, *aire*-deficient, IRBP-deficient (DKO) mice do develop autoimmune disease characterized by mononuclear infiltrates directed against other organs, including the salivary and lacrimal glands (Fig. 4 B and Fig. S7), and autoantibodies specific for antigens in the stomach, salivary and lacrimal glands, and prostate (Fig. 4 D), thus ruling out a nonspecific effect of the IRBP knockout mutation in suppressing autoimmunity. In addition, the cellular infiltrate of the eye was analyzed by flow cytometry using markers specific for CD4⁺ T cells (Fig. 4 F and Fig. S8). CD4⁺ T cells were observed in the eyes of *aire*-deficient, IRBP-sufficient animals but not in the eyes of *aire*/IRBP double-deficient mice.

Absence of IRBP within the thymus is sufficient to induce spontaneous autoimmunity

Given that IRBP appears to be such a dominant antigen despite *aire*'s thymic regulation of several retina-specific genes, we next sought to determine if the absence of IRBP within the thymic compartment alone is sufficient to cause spontaneous autoimmune uveitis. For this, we performed thymic transfers of IRBP-deficient, *aire*-sufficient fetal thymic stroma under the kidney capsule of nude mice (which are both IRBP and *aire* sufficient) and next aged recipients

layer, as shown in representative staining. Both sets of animals had autoantibodies present against other organs, summarized in (D), where circles/numbers represent individual mice and red-shaded wedges represent positive staining for a particular autoantibody. (E) Immunoblotting of whole-eye extracts prepared from immunodeficient scid animals with sera from 18–20-wk-old *aire*-deficient, IRBP-deficient, or *aire*- and IRBP-deficient animals in the C57BL/6 background. (F) Flow cytometry was used to assess the presence or absence of CD4⁺ T cells within the retina. Ocular cells from *aire*-deficient, IRBP-sufficient (thin black line), *aire*-deficient/IRBP-deficient (DKO; thick black line), or C57BL/6 wild-type (red line) mice were gated on lymphocytes and stained with CD4.

for 10 wk to determine if they could develop autoimmune disease of the eye. As shown in Fig. 5 A, all five recipients of IRBP-deficient thymi spontaneously developed autoantibodies to the retina, whereas no autoantibodies were observed in any of the five mice that received IRBP-sufficient thymic stroma. Histological evaluation revealed a mononuclear infiltrate in the retina of recipients of IRBP-deficient thymic stroma (Fig. 5 B). Finally, flow cytometry was used to confirm the presence of CD4⁺ T cells within the eye of IRBP-deficient, but not IRBP-sufficient, thymic stroma recipients (Fig. 5 C and Fig. S9, available at <http://www.jem.org/cgi/content/full/jem.20061864/DC1>).

DISCUSSION

We have demonstrated that the loss of expression of a single self-antigen exclusively within the thymus can induce a spontaneous organ-specific autoimmune attack, even in the presence of functional Aire. This result suggests that there are individual TSAs whose thymic expression is crucial in preventing autoimmune disease. Previous studies have suggested the importance of thymic tolerance and thymic TSA expression as a component in disease susceptibility (23–26), but to our knowledge no previous study has demonstrated that the loss of a single TSA in the thymus is sufficient to induce organ-specific autoimmunity in a host with a polyclonal T cell repertoire. Unlike our results described in this paper, recent experiments with proinsulin 2 indicated that deficiency of this gene within the thymic compartment was not sufficient to induce diabetes (27). In the case of insulin, peripheral tolerance mechanisms were likely sufficient to prevent overt autoimmunity, because a defect in central tolerance could be detected through an increase in insulin-specific T cells. In contrast, our results have identified an antigen for which central tolerance is critically important. It will be interesting to determine whether or not the phenomenon described in this paper is restricted to the eye. It is possible that we may have obtained this result because we focused on a site that has been described as immunologically privileged (28). Perhaps because the immune system has limited access to the eye, there may be limited opportunity to induce tolerance via peripheral mechanisms, and this could increase the importance of central tolerance mechanisms for this target organ.

The level of IRBP expression within the thymus in our experiments was remarkably low. Despite this low level of expression, it is clearly enough to help impose tolerance in our model system, most likely through mechanisms that involve deletion rather than the positive selection of regulatory cells; in previous experiments, cotransfers of equal amounts of wild-type and aire-deficient thymi or lymphocytes were not capable of suppressing retinal disease (9). Furthermore, it has been shown that T reg cells capable of suppressing EAU can be generated even in the absence of IRBP (29). It remains to be understood how even this low level of expression allows for sufficient presentation to the developing thymocyte repertoire. Interestingly, because we could induce uveitis with transfers of IRBP-deficient/aire-sufficient

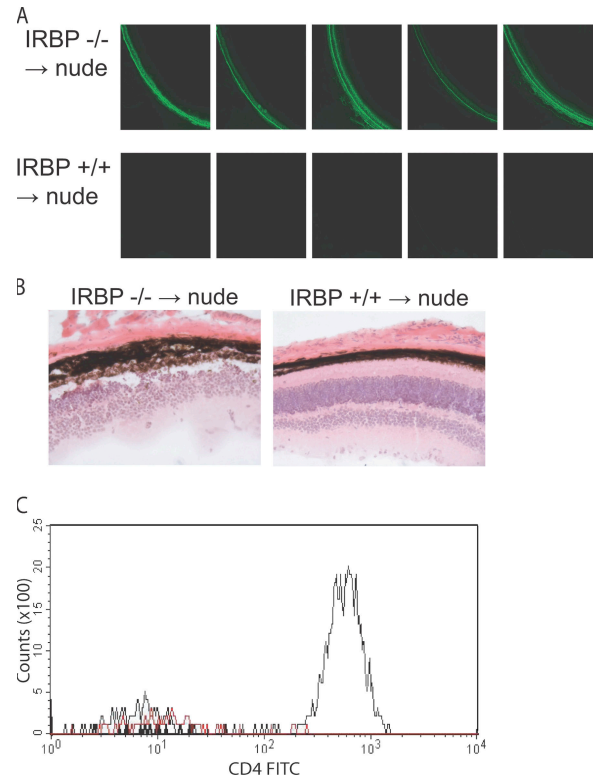


Figure 5. The absence of IRBP within the thymic compartment is, by itself, sufficient for autoimmunity. Thymi from IRBP-deficient or wild-type control mice in the C57BL/6 background were isolated and cultured for 8 d in 2-deoxyguanosine to deplete hematopoietic cells. Thymic stroma was then transferred to individual C57BL/6 nude congenic recipients ($n = 5$ for recipients in each group) under the kidney capsule. (A) Reconstituted mice were aged 12 wk after transfer and were analyzed for the presence of eye-specific autoantibodies by indirect immunofluorescence. (B) Hematoxylin and eosin-stained sections from recipients of IRBP-sufficient or IRBP-deficient thymic stroma. (C) Flow cytometry was used to assess the presence or absence of CD4⁺ T cells within the retina of nude recipients. Ocular cells from IRBP-deficient thymic stroma recipients (thin black line), IRBP-sufficient thymic stroma recipients (DKO; thick black line), or C57BL/6 wild-type (red line) mice were gated on lymphocytes and stained with CD4.

thymic stroma, this process appears to be exclusively dependent on IRBP's expression and not another possible activity of Aire such as antigen presentation, as invoked in a recent study (9).

We have also confirmed one mechanism by which Aire operates to maintain self-tolerance. One of the current models for the function of Aire in maintaining self-tolerance has been that it is involved in the regulation of TSA expression in the thymus and that the loss of this function leads to a defect in negative selection of autoreactive thymocytes (3, 4, 12). Microarray analysis of mTEC expression in the presence or absence of Aire has helped identify many potential targets for autoimmunity in the Aire-deficient model (3, 13), but data have been lacking on the actual primary targets to date. Two recent studies identified autoantigens targeted in the

salivary gland and exocrine pancreas (30, 31) in the *aire*-deficient model whose expression was not regulated by *aire* in the thymus. However, these studies did not exclude epitope spreading as an explanation for their results. In contrast, through the use of IRBP/*aire* double-deficient animals, we have strong evidence that IRBP is the primary antigen driving the uveitis in these animals and is not an autoantigen by virtue of a secondary process like epitope spreading. These data help confirm the link between *aire*-driven regulation of TSA expression in the thymus and the development of a spontaneous autoimmune disease in animals with a polyclonal T cell repertoire. Our findings have also identified and confirmed that a single antigen is the primary target in a spontaneous autoimmune disease, something that has been extremely difficult to demonstrate in other spontaneous infiltrative autoimmune diseases, perhaps with the exception of insulin as a target in the NOD mouse model of diabetes (32).

Interestingly, IRBP was not a predictable eye antigen in our model using the current mTEC expression profiling data (Fig. 3). Upon surveying the existing mTEC expression profiling data, we discovered that IRBP was not present on the microarrays used in these studies. This result suggests that there are many potential TSAs expressed in mTECs in an *aire*-dependent fashion that may be immunologically relevant but are not observed using the existing microarray analyses. Why IRBP is such a dominant and potent antigen in this system remains unclear. Our work suggests that there are properties of IRBP yet to be identified that make it immunogenic, which could include such processes as differential splicing, posttranslational modification, or antigen trafficking within and perhaps out of the eye. Along these lines, we also cannot completely exclude that the protective effect against eye autoimmunity in *aire*-deficient/IRBP-deficient animals is caused by secondary effects of the IRBP knockout that make the eye less immunogenic. Further work on IRBP as an autoantigen should shed light on the uveitic process that occurs both in these mice and in IRBP-induced EAU. IRBP is a large protein with multiple potentially immunogenic epitopes. However, it is not clear how and where IRBP peptides are presented to autoreactive cells. If priming occurs in the draining lymph nodes, by what route do IRBP-specific T cells gain access to the retina? A more detailed understanding of IRBP and IRBP-specific T cell responses should help elucidate additional aspects of disease pathogenesis and progression.

It is also tempting to speculate that susceptibility to EAU depends on a variation in IRBP expression within the thymic compartment across strains. In the EAU model, there are clearly strains that are resistant, protective, and susceptible. In our colony, both the EAU-resistant C57BL/6 and EAU-protected BALB/c strains are susceptible to spontaneous uveitis when deficient for *aire* (unpublished data) (3). This leaves open the possibility that when IRBP is removed from the thymus by *aire* deficiency, the strain dependency for EAU is removed; in fact, there are data to support strain differences in eye antigen expression in the thymus (33, 34).

Collectively, our results show that thymic tolerance can be crucial in preventing autoimmune disease and that even the loss of expression of a single TSA in the thymus can generate spontaneous autoimmunity. It will be interesting to identify other thymic TSAs that behave similarly to IRBP and also determine if this observation is applicable to autoimmunity in human subjects given the link to the APECED syndrome.

MATERIALS AND METHODS

Mice. *Aire*-deficient mice were generated as previously described (3), and IRBP-deficient mice in the C57BL/6 background (>10 generations) were provided by R. Caspi (22). *Aire*-deficient mice used in these experiments were backcrossed into the C57BL/6, BALB/c, and NOD Lt/J backgrounds >10 generations. C57BL/6 × NOD Lt/J F2 *aire*-deficient mice came from intercrosses of C57BL/6 and NOD Lt/J *aire*-deficient mice. All mice were housed in a pathogen-free barrier facility at the University of California, San Francisco (UCSF). Experiments complied with the Animal Welfare Act and NIH guidelines for the ethical care and use of animals in biomedical research and were approved by the UCSF Animal Care and Use Committee.

Antigens and reagents. IRBP was isolated from bovine retinas, as described previously, using Con A-sepharose affinity chromatography and fast performance liquid chromatography (35). Bovine S-Ag (arrestin) was prepared from the ConA column flowthrough as described previously (36).

Histology. Organs from mice were harvested and fixed overnight in 10% formalin, embedded in paraffin, sectioned, and stained for hematoxylin and eosin. Immune infiltrates of organs were confirmed by an independent reading of the slides with a blinded observer.

Immunoprecipitation. Immunoprecipitation of autoantigens was performed using protein G agarose coupled to *aire*-sufficient or *aire*-deficient sera as described previously (17). In brief, tissue extracts were prepared from immunodeficient mouse eyes homogenized in 0.15 M NaCl, 0.05 M Tris (pH 8), and 0.1% CHAPS (Sigma-Aldrich). Protein agarose G-coupled columns were washed in 30 mL PBS, and tissue extracts from immunodeficient animals prepared in CHAPS buffer were passed through the matrix. Columns were washed with 30 mL PBS and washed again with 30 mL of 10 mM phosphate, pH 6.8. Eluates were collected by passing 0.5 ml of 100 mM glycine, pH 2.5, over the column and collecting the flowthrough. Eluates from multiple runs were pooled and concentrated in a centrifugal protein concentrator (Vivaspin; Sartorius).

Immunoblotting. Sera were screened for the presence of autoantibodies by Western blotting as previously described (10). For competition studies, sera were preincubated with serial dilutions of full-length bovine IRBP or S-Ag in TBS-T with 5% nonfat dry milk for 2 h at room temperature before use as the primary reagent. The concentrations used were 30 μ g (highest), 3 μ g, 300 ng, 30 ng, 3 ng, and 0.3 ng (lowest) of purified bovine protein.

In-gel digestion and PMF. IRBP was identified by provisional PMF as previously described (37–40). In brief, gel bands were excised, destained (stain-stripped) three times in 50% acetonitrile and 25 mM ammonium bicarbonate (pH 8), dehydrated with 100% acetonitrile, and dried in a Speed-Vac (Savant). Gel pieces were rehydrated with a solution of sequencing grade trypsin (10 μ g trypsin [Promega]/ml in 25 mM ammonium bicarbonate), and the digestion was performed for 16 h at 37°C. Peptides were extracted three times by the addition of two volumes of an aqueous solution of 50% acetonitrile and 5% trifluoroacetic acid. The extracts were combined and reduced to a final volume of 5–10 μ l. PMF was used for preliminary protein identification. Portions (typically 5%) of the unseparated tryptic digest was cocrystallized in a matrix of 5 mg/ml α -cyano-4-hydroxycinnamic acid and analyzed on a MALDI-TOF mass spectrometer (Voyager-DE STR; Applied Biosystems) operating in reflector mode. Mass spectra were produced

representing protonated molecular ions (MH^+) of tryptic peptides from the proteins present in each gel spot. The mass spectra were internally mass calibrated using two trypsin autolysis products present in the digest mixture (842.51 and 2,211.1046 D, respectively). The mass measurement accuracy for all peptides was ± 25 ppm, and the mass measurement precision, defined as the standard deviation of differences between the experimental and theoretical peptide masses, was typically ≤ 25 ppm. Preliminary protein identities were established by matching the experimentally determined peptide masses to those produced by an *in silico* tryptic digestion of the Swiss-Prot protein database (available at <http://us.expasy.org>) within the window of experimental mass measurement accuracy. The PMF data-searching algorithm (available through MS-Fit at <http://prospector.ucsf.edu>) was used to perform the database searches.

Autoantibodies and indirect immunofluorescence. Sera were prepared from tail-vein bleeds or at the time of death. Autoantibodies for the eye were detected by indirect immunofluorescence as described previously (3). Slides were examined on a microscope (Axiostar; Carl Zeiss MicroImaging, Inc.) with 10 \times , 20 \times , and 40 \times lenses. Images were obtained using an AxioCam with AxioVision software (both from Carl Zeiss MicroImaging, Inc.).

Immunostaining. Immune cell subtypes were visualized by immunohistochemistry using antibodies specific for CD4, CD8, and IgD (BD Biosciences) and a DAB staining kit (Vector Laboratories).

Adoptive transfer. Cervical lymph node cells and splenocytes were harvested, and CD4 $^+$ or CD8 $^+$ T cells were depleted using complement. Cell populations (5×10^6 CD4 $^+$ and CD8 $^+$, CD4 $^+$ depleted, or CD8 $^+$ depleted) were injected *i.v.* into NOD.*scl*d mice. On days 0, 5, 19, and 33, animals were treated with 0.5 mg/mouse of anti-CD4 (GK1.5, CD4 $^+$ depleted) or anti-CD8 (YTS169.4, CD8 depleted) to remove residual CD4 $^+$ or CD8 $^+$ T cells (41). Animals were aged 40 d after transfer, then killed and analyzed as described in the figures.

ELISPOT analysis. CD4 $^+$ T cells from *aire*-deficient or *aire* wild-type C57BL/6 mice were isolated by AutoMACS (Miltenyi Biotec) using a CD4-specific antibody (GK1.5; Southern Biotechnology Associates, Inc.). The release of IFN- γ by CD4 T cells was measured by ELISPOT assay. In brief, plates (Immunospot M200; BD Biosciences) were coated with 2 μ g/ml of anti-mouse IFN- γ mAb (BD Biosciences) and incubated overnight at 4°C. The plates were washed with PBS and blocked with medium containing 10% FCS for 2 h at 37°C. 125,000 effector CD4 $^+$ T cells and 25,000 irradiated (3,000 rad) APCs were added to each well and incubated for 24 h in RPMI 1640 complete medium. The plates were washed thoroughly with PBS before adding 2 μ g/ml of biotin-labeled IFN- γ mAb (2 μ g/ml; BD Biosciences) and incubating overnight at 4°C. After further incubation with avidin-horseradish peroxidase (1:100 dilutions; BD Biosciences) for 1 h at room temperature, the plates were developed using substrate solution (AEC; BD Biosciences). Positive spots displayed in the plate membranes were examined using an ELISPOT reader system (Transtec; Cell Technology). The number of spot-forming cells was the average number of spots in duplicate wells.

Thymic stroma preparation. TECs were prepared according to a previously established protocol (42).

Real-time PCR. Real-time PCR was performed on cDNA prepared from DNase-treated RNA. *Aire*, *insulin*, and *cyclophilin* primers were used as previously described (3, 9). For IRBP, the following primers were used: forward, 5'-AATGACTCGGTCAGCGAACTTT-3'; reverse, 5'-CTGTC-ACACCACTGGTTCAGGAT-3'; and probe, FAM-ACAGGTGAACGAT-ATGGCTCCAAGAAG-TAMRA. Additional primer and probe sequences are listed in Table S2, available at <http://www.jem.org/cgi/content/full/jem.20061864/DC1>. Reactions were run on a sequence detection system machine (HT7900; Applied Biosystems). For analysis of target gene expression from organ-derived cDNA, the standard curve method was used.

Microarray analysis. *Aire*-dependent transcripts were determined by microarray analysis of wild-type and *aire*-deficient thymic stroma. Two independent and previously published microarray datasets were analyzed (3, 13). Microarray data are available in the National Center for Biotechnology Information Gene Expression Omnibus (<http://www.ncbi.nlm.nih.gov/geo/>) under accession nos. GSE85, GSE2585, and GSE3023. The list of *aire*-regulated genes was further refined by including only those genes that were determined to be expressed in the retinal compartment of the eye (21).

Flow cytometry. Eyes were incubated in 2 mg/ml collagenase D in RPMI 1640 supplemented with 2% fetal calf serum for 2 h. The remaining tissue was dispersed by vortexing and filtered through nylon mesh. Cells were stained with antibodies specific for the CD4 surface marker (BD Biosciences). Cells were analyzed on a FACSCalibur (Becton Dickinson).

Thymic transplants. Thymi were isolated from newborn IRBP-deficient or wild-type mice and cultured in 1.35 mM 2-deoxyguanosine (Sigma-Aldrich) for 6–8 d to deplete bone marrow-derived cells. The thymi were washed in media for 2 h and transplanted under the kidney capsule of 6–8-wk-old adult nude mice on the C57BL/6 background (The Jackson Laboratory). 12 wk after transplantation, whole blood and serum were collected. T cell reconstitution of all transplanted mice was confirmed by FACS analysis of whole blood for CD4, CD8, and CD3. Sera was analyzed for autoantibodies by indirect immunofluorescence.

Statistics. Data were analyzed using Prism software (GraphPad). For ELISPOT analysis, a nonparametric two-tailed Mann-Whitney test was applied, with an α level of 0.05 ($n = 7$ for *aire*-sufficient and *aire*-deficient animals). For histological analysis of *aire*-deficient versus *aire*/IRBP-deficient animals, a log-rank sum test was applied, with an α level of 0.05 ($n = 9$ and 7 for *aire*-deficient and *aire*/IRBP-deficient animals, respectively).

Online Supplemental Material. Supplemental materials and methods provides information about Western blotting, immunofluorescence, immunostaining, thymic stroma preparation, and microarray analysis. Table S1 details the cell populations used in the adoptive transfer experiments depicted in Fig. 2. Table S2 provides sequences for the quantitative real-time PCR primers and probes used in the paper. Fig. S1 provides confirmatory data for the immunoreactivity of IRBP using an additional background of mice (intercrossed B6 \times NOD F2). Figs. S2–S4 show the immunoblotting of immunoaffinity-purified material that was sent to mass spectrometry, the specific peptides identified by mass spectrometry, and confirm that the 150-kD band in *aire*-deficient sera recognizes IRBP using indirect immunofluorescence. Fig. S5 shows that there is no difference between *aire*-sufficient and *aire*-deficient APCs. Fig. S6 depicts the penetrance of ocular autoimmunity in C57BL/6 *aire*-deficient animals. Fig. S7 shows spontaneous autoimmunity in other organs of *aire*/IRBP double-deficient animals, demonstrating that the effect is eye specific. Fig. S8 depicts the presence of lymphocytes in the eyes of *aire*-deficient but not *aire*/IRBP double-deficient animals. Fig. S9 shows the presence of lymphocytes in the eyes of nude recipients of IRBP-deficient, but not IRBP-sufficient, thymic stroma. Online supplemental material is available at <http://www.jem.org/cgi/content/full/jem.20061864/DC1>.

We thank J. Bluestone, A. Abbas, J. Gardner, M. Su, A. Shum, and M. Cheng for critical review of the manuscript; members of the Anderson Laboratory for helpful discussions; and the UCSF Biomolecular Resource Center Mass Spectrometry Facility for mass spectrometry.

This work was supported by grants from the NIH (DK59958 and EY016408), the Pew Scholars Program in the Biomedical Sciences, the Sandler Foundation, and the Giannini Foundation. The UCSF Biomolecular Resource Center Mass Spectrometry Facility is supported by a grant from the Sandler Family Foundation.

The authors have no conflicting financial interests.

Submitted: 30 August 2006

Accepted: 26 October 2006

REFERENCES

- Kappler, J.W., N. Roehm, and P. Marrack. 1987. T cell tolerance by clonal elimination in the thymus. *Cell*. 49:273–280.
- Kisielow, P., H. Bluthmann, U.D. Staerz, M. Steinmetz, and H. von Boehmer. 1988. Tolerance in T-cell-receptor transgenic mice involves deletion of nonmature CD4+8+ thymocytes. *Nature*. 333:742–746.
- Anderson, M.S., E.S. Venanzi, L. Klein, Z. Chen, S.P. Berzins, S.J. Turley, H. von Boehmer, R. Bronson, A. Dierich, C. Benoist, and D. Mathis. 2002. Projection of an immunological self shadow within the thymus by the aire protein. *Science*. 298:1395–1401.
- Liston, A., S. Lesage, J. Wilson, L. Peltonen, and C.C. Goodnow. 2003. Aire regulates negative selection of organ-specific T cells. *Nat. Immunol.* 4:350–354.
- Nagamine, K., P. Peterson, H.S. Scott, J. Kudoh, S. Minoshima, M. Heino, K.J. Krohn, M.D. Laloti, P.E. Mullis, S.E. Antonarakis, et al. 1997. Positional cloning of the APECED gene. *Nat. Genet.* 17:393–398.
- The Finnish-German APECED Consortium. 1997. An autoimmune disease, APECED, caused by mutations in a novel gene featuring two PHD-type zinc-finger domains. Autoimmune Polyendocrinopathy-Candidiasis-Ectodermal Dystrophy. *Nat. Genet.* 17:399–403.
- Perheentupa, J. 2006. Autoimmune polyendocrinopathy-candidiasis-ectodermal dystrophy. *J. Clin. Endocrinol. Metab.* 91:2843–2850.
- Ramsey, C., O. Winqvist, L. Puhakka, M. Halonen, A. Moro, O. Kampe, P. Eskelin, M. Peltö-Huikko, and L. Peltonen. 2002. Aire deficient mice develop multiple features of APECED phenotype and show altered immune response. *Hum. Mol. Genet.* 11:397–409.
- Anderson, M.S., E.S. Venanzi, Z. Chen, S.P. Berzins, C. Benoist, and D. Mathis. 2005. The cellular mechanism of Aire control of T cell tolerance. *Immunity*. 23:227–239.
- Jiang, W., M.S. Anderson, R. Bronson, D. Mathis, and C. Benoist. 2005. Modifier loci condition autoimmunity provoked by Aire deficiency. *J. Exp. Med.* 202:805–815.
- Derbinski, J., A. Schulte, B. Kyewski, and L. Klein. 2001. Promiscuous gene expression in medullary thymic epithelial cells mirrors the peripheral self. *Nat. Immunol.* 2:1032–1039.
- Su, M.A., and M.S. Anderson. 2004. Aire: an update. *Curr. Opin. Immunol.* 16:746–752.
- Derbinski, J., J. Gabler, B. Brors, S. Tierling, S. Jonnakuty, M. Hergenhanh, L. Peltonen, J. Walter, and B. Kyewski. 2005. Promiscuous gene expression in thymic epithelial cells is regulated at multiple levels. *J. Exp. Med.* 202:33–45.
- Caspi, R.R. 1999. Immune mechanisms in uveitis. *Springer Semin. Immunopathol.* 21:113–124.
- Chan, C.C., R.B. Nussenblatt, B. Wiggert, T.M. Redmond, L.S. Fujikawa, G.J. Chader, and I. Gery. 1987. Immunohistochemical analysis of experimental autoimmune uveoretinitis (EAU) induced by interphotoreceptor retinoid-binding protein (IRBP) in the rat. *Immunol. Invest.* 16:63–74.
- Perheentupa, J. 2006. Autoimmune polyendocrinopathy-candidiasis-ectodermal dystrophy. *J. Clin. Endocrinol. Metab.* 91:2843–2850.
- Harlow, E., and D. Lane. 1999. Using Antibodies: A Laboratory Manual. Cold Spring Harbor Laboratory Press, Cold Spring Harbor, NY. 495 pp.
- Gery, I., R.B. Nussenblatt, C.C. Chan, and R.R. Caspi. 2002. Autoimmune diseases of the eye. In *The Molecular Pathology of Autoimmune Diseases*. A.N. Theophilopoulos and C.A. Bona, editors. Taylor and Francis, New York. 1665–1676.
- Ramsey, C., S. Hassler, P. Marits, O. Kampe, C.D. Surh, L. Peltonen, and O. Winqvist. 2006. Increased antigen presenting cell-mediated T cell activation in mice and patients without the autoimmune regulator. *Eur. J. Immunol.* 36:305–317.
- Kyewski, B., J. Derbinski, J. Gotter, and L. Klein. 2002. Promiscuous gene expression and central T-cell tolerance: more than meets the eye. *Trends Immunol.* 23:364–371.
- Diehn, J.J., M. Diehn, M.F. Marmor, and P.O. Brown. 2005. Differential gene expression in anatomical compartments of the human eye. *Genome Biol.* 6:R74.
- Liou, G.I., Y. Fei, N.S. Peachey, S. Matragoon, S. Wei, W.S. Blamer, Y. Wang, C. Liu, M.E. Gottesman, and H. Ripps. 1998. Early onset photoreceptor abnormalities induced by targeted disruption of the interphotoreceptor retinoid-binding protein gene. *J. Neurosci.* 18:4511–4520.
- Avichezer, D., R.S. Grajewski, C.C. Chan, M.J. Mattapallil, P.B. Silver, J.A. Raber, G.I. Liou, B. Wiggert, G.M. Lewis, L.A. Donoso, and R.R. Caspi. 2003. An immunologically privileged retinal antigen elicits tolerance: major role for central selection mechanisms. *J. Exp. Med.* 198:1665–1676.
- Thebault-Baumont, K., D. Dubois-Laforgue, P. Krief, J.P. Briand, P. Halbout, K. Vallon-Geoffrey, J. Morin, V. Laloux, A. Lehuen, J.C. Carel, et al. 2003. Acceleration of type 1 diabetes mellitus in proinsulin 2-deficient NOD mice. *J. Clin. Invest.* 111:851–857.
- Huseby, E.S., B. Sather, P.G. Huseby, and J. Goverman. 2001. Age-dependent T cell tolerance and autoimmunity to myelin basic protein. *Immunity*. 14:471–481.
- Klein, L., M. Klugmann, K.A. Nave, V.K. Tuohy, and B. Kyewski. 2000. Shaping of the autoreactive T-cell repertoire by a splice variant of self protein expressed in thymic epithelial cells. *Nat. Med.* 6:56–61.
- Faideau, B., C. Lotton, B. Lucas, I. Tardivel, J.F. Elliott, C. Boitard, and J.C. Carel. 2006. Tolerance to proinsulin-2 is due to radioresistant thymic cells. *J. Immunol.* 177:53–60.
- Streilein, J.W. 2003. Ocular immune privilege: therapeutic opportunities from an experiment of nature. *Nat. Rev. Immunol.* 3:879–889.
- Grajewski, R.S., P.B. Silver, R.K. Agarwal, S.B. Su, C.C. Chan, G.I. Liou, and R.R. Caspi. 2006. Endogenous IRBP can be dispensable for generation of natural CD4+CD25+ regulatory T cells that protect from IRBP-induced retinal autoimmunity. *J. Exp. Med.* 203:851–856.
- Niki, S., K. Oshikawa, Y. Mouri, F. Hirota, A. Matsushima, M. Yano, H. Han, Y. Bando, K. Izumi, M. Matsumoto, et al. 2006. Alteration of intra-pancreatic target-organ specificity by abrogation of Aire in NOD mice. *J. Clin. Invest.* 116:1292–1301.
- Kuroda, N., T. Mitani, N. Takeda, N. Ishimaru, R. Arakaki, Y. Hayashi, Y. Bando, K. Izumi, T. Takahashi, T. Nomura, et al. 2005. Development of autoimmunity against transcriptionally unrepressed target antigen in the thymus of Aire-deficient mice. *J. Immunol.* 174:1862–1870.
- Nakayama, M., N. Abiru, H. Moriyama, N. Babaya, E. Liu, D. Miao, L. Yu, D.R. Wegmann, J.C. Hutton, J.F. Elliott, and G.S. Eisenbarth. 2005. Prime role for an insulin epitope in the development of type 1 diabetes in NOD mice. *Nature*. 435:220–223.
- Egwuagu, C.E., P. Charukamnoetkanok, and I. Gery. 1997. Thymic expression of autoantigens correlates with resistance to autoimmune disease. *J. Immunol.* 159:3109–3112.
- Charukamnoetkanok, P., A. Fukushima, S.M. Whitcup, I. Gery, and C.E. Egwuagu. 1998. Expression of ocular autoantigens in the mouse thymus. *Curr. Eye Res.* 17:788–792.
- Pepperberg, D.R., T.L. Okajima, H. Ripps, G.J. Chader, and B. Wiggert. 1991. Functional properties of interphotoreceptor retinoid-binding protein. *Photochem. Photobiol.* 54:1057–1060.
- Pennesi, G., M.J. Mattapallil, S.H. Sun, D. Avichezer, P.B. Silver, Z. Karabekian, C.S. David, P.A. Hargrave, J.H. McDowell, W.C. Smith, et al. 2003. A humanized model of experimental autoimmune uveitis in HLA class II transgenic mice. *J. Clin. Invest.* 111:1171–1180.
- Henzel, W.J., T.M. Billeci, J.T. Stults, S.C. Wong, C. Grimley, and C. Watanabe. 1993. Identifying proteins from two-dimensional gels by molecular mass searching of peptide fragments in protein sequence databases. *Proc. Natl. Acad. Sci. USA.* 90:5011–5015.
- James, P., M. Quadroni, E. Carafoli, and G. Gonnert. 1993. Protein identification by mass profile fingerprinting. *Biochem. Biophys. Res. Commun.* 195:58–64.
- Pappin, D.J., P. Hojrup, and A.J. Bleasby. 1993. Rapid identification of proteins by peptide-mass fingerprinting. *Curr. Biol.* 3:327–332.
- Yates, J.R., III, S. Speicher, P.R. Griffin, and T. Hunkapiller. 1993. Peptide mass maps: a highly informative approach to protein identification. *Anal. Biochem.* 214:397–408.
- Yin, D.P., L.L. Ma, H.N. Sankary, J. Shen, H. Zeng, A. Varghese, and A.S. Chong. 2002. Role of CD4+ and CD8+ T cells in the rejection of concordant pancreas xenografts. *Transplantation.* 74:1236–1241.
- Gray, D.H., A.P. Chidgey, and R.L. Boyd. 2002. Analysis of thymic stromal cell populations using flow cytometry. *J. Immunol. Methods.* 260:15–28.